UNCLASSIFIED
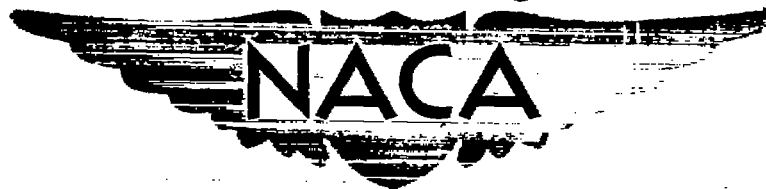
NACA

RESEARCH MEMORANDUM

INVESTIGATION OF LOW-SPEED LATERAL CONTROL AND

HINGE-MOMENT CHARACTERISTICS OF A 20-PERCENT-CHORD PLAIN

AILERON ON A 47.7° SWEPTBACK WING OF ASPECT RATIO 5.1 AT

A REYNOLDS NUMBER OF 6.0 × 10⁶

By William M. Hadaway and Reino J. Salmi

Langley Aeronautical Laboratory
Langley Field, Va.

CLASSIFICATION CANCELLED

FOR REFERENCE

Authority _G. W. Crowley_ Date _12/11/53_
_EC. 1050.1_

By _J.H. 1-7-54_ See _naca_

NOT TO BE TAKEN FROM THIS ROOM

CLASSIFIED DOCUMENT

_RE 1811_

NATIONAL ADVISORY COMMITTEE
FOR AERONAUTICS
WASHINGTON
October 22, 1951

UNCLASSIFIED

NATIONAL ADVISORY COMMITTEE FOR AERONAUTICS

RESEARCH MEMORANDUM

INVESTIGATION OF LOW-SPEED LATERAL CONTROL AND

HINGE-MOMENT CHARACTERISTICS OF A 20-PERCENT-CHORD PLAIN

AILERON ON A 47.7° SWEPTBACK WING OF ASPECT RATIO 5.1 AT

A REYNOLDS NUMBER OF 6.0×10^6

By William M. Hadaway and Reino J. Salmi

SUMMARY

The low-speed lateral control and hinge-moment characteristics of a 20-percent-chord plain aileron on a 47.7° sweptback wing of aspect ratio 5.1 have been determined in the Langley 19-foot pressure tunnel. The tests were made with and without high-lift and stall-control devices at a Reynolds number of 6.0×10^6.

The results indicated that an airplane with a wing similar to the one tested may exhibit undesirable rolling oscillations and vibrations at moderate and high angles of attack due to intermittent separation of flow over the wing. The static rolling moments obtained with large aileron deflections were greater in magnitude, however, than the rolling moments induced by the separated flow, thereby indicating that some degree of lateral control could be maintained. At zero angle of attack, a rate of change of rolling-moment coefficient with aileron deflec-tion C_{l_δ} of 0.00080 was obtained which was in fair agreement with the calculated value. The addition of leading- and trailing-edge flaps did not appreciably affect C_{l_δ} at low lift coefficients. Because of the nonlinear characteristics of the rolling-moment data, the value of the aileron effectiveness parameter C_{l_δ} was not well-defined in the angle-of-attack range through which flow separation occurred. However, the data indicated that the rolling moments near maximum lift were about 70 percent of the values obtained at zero angle of attack for large total aileron deflections. Measurements of the aileron hinge moments and balance-chamber pressures indicated that a ratio of the aileron nose balance to the aileron chord of 0.60 or more will be required to balance completely the internally sealed type of aileron.

INTRODUCTION

Previous investigations of plain flap-type ailerons on sweptback
wings (references 1 to 3) have shown that the aileron effectiveness in
the low lift range can be predicted by semiempirical means based on
simple sweep theory. The effectiveness of the aileron at the higher
lift coefficients, however, cannot be calculated because of the early
separation of flow over the wing (reference 4). An investigation was
made on a 47.7° sweptback wing of aspect ratio 5.1 employing a 20-percent-
chord outboard aileron to provide information on the aileron effectiveness
on a wing of relatively higher aspect ratio and sweep than has previously
been investigated. The tests were made at a Reynolds number of 6.0×10^6
and a Mach number of 0.14. These tests are part of a general investigation
of the subject wing and the longitudinal stability characteristics have
been reported in references 4 to 6.

SYMBOLS

All data are referred to a system of wind axes originating at the
quarter-chord point of the mean aerodynamic chord projected to the
plane of symmetry. Symbols used herein are defined as follows:

C_L lift coefficient $\left(\dfrac{\text{Lift}}{qS}\right)$

C_m pitching-moment coefficient $\left(\dfrac{\text{Pitching moment}}{qS\bar{c}}\right)$

C_n yawing-moment coefficient $\left(\dfrac{\text{Yawing moment}}{qSb}\right)$

C_l rolling-moment coefficient $\left(\dfrac{\text{Rolling moment}}{qSb}\right)$

C_{h_a} aileron hinge-moment coefficient $\left(\dfrac{\text{Hinge moment}}{2M_a q}\right)$

C_{Z_a} aileron-load coefficient $\left(\dfrac{Z}{qS_a}\right)$

Z aileron load normal to wing chord line, pounds

P_R resultant pressure coefficient in aileron balance compartment $\left(\dfrac{\text{Pressure below seal} - \text{Pressure above seal}}{q}\right)$

E aileron-seal leakage factor $\left(1 - \dfrac{\text{Pressure difference across seal}}{\text{Pressure difference across vents}}\right)$

R Reynolds number $\left(\dfrac{\rho V \bar{c}}{\mu}\right)$

α angle of attack of root chord line, degrees

δ_a aileron deflection measured in plane perpendicular to hinge line, positive when deflected down, degrees

S wing area (30.35 sq ft)

S_a aileron area rearward of hinge line (0.7120 sq ft)

c local wing chord measured parallel to plane of symmetry, feet

$\bar{c}$ mean aerodynamic chord (2.60 ft) $\left(\dfrac{2}{S}\displaystyle\int_0^{b/2} c^2 dy\right)$

c' local wing chord measured perpendicular to 0.286 chord line

c_a aileron chord measured normal to the 0.286 chord line

$\bar{c}_a$ root-mean-square chord of aileron behind and normal to hinge line

$\bar{c}_b$ root-mean-square chord of assumed aileron balance measured forward of and normal to aileron hinge line

q dynamic pressure, pounds per square foot $\left(\dfrac{\rho V^2}{2}\right)$

b wing span perpendicular to plane of symmetry (12.46 ft)

M_a moment area of aileron behind hinge line about hinge axis

$\quad$ (0.0913 cu ft) $\left(\dfrac{1}{2} \displaystyle\int_0^{b_a} c_a{}^2 dy \right)$

b_a aileron span measured parallel to aileron hinge line (33.82 in.)

ρ mass density, slugs per cubic foot

V free-stream velocity, feet per second

μ coefficient of viscosity, slugs per foot second

y lateral coordinate, feet

$\delta_{a_{total}} = \Delta\delta_a$ arithmetical sum of equal up and down aileron deflections for an assumed set of ailerons, degrees

$\left(\Delta\alpha\right)_p$ angle-of-attack change due to rolling

C_{l_δ} rate of change of rolling-moment coefficient with aileron deflection

C_{h_δ} rate of change of aileron hinge-moment coefficient with aileron deflection

C_{h_α} rate of change of aileron hinge-moment coefficient with angle of attack

P_{R_δ} rate of change of resultant pressure coefficient with aileron deflection

P_{R_α} rate of change of resultant pressure coefficient with angle of attack

$C_{h_\delta}{}'$ rate of change of aileron hinge-moment coefficient in steady roll with aileron deflection

C_{l_p} damping coefficient, that is, rate of change of rolling-moment coefficient C_l with wing tip-helix angle $pb/2V$

p angular velocity in roll, radians per second

MODEL .

The model used in the investigation was of steel construction and had a leading-edge sweep of 47.7°, an aspect ratio of 5.1, a taper ratio of 0.383, and NACA 64-210 airfoil sections normal to the 0.286 chord line. Washout about the 0.286 chord line was 1.32° and there was no dihedral. The general dimensions of the model are presented in figure 1.

The left wing was fitted with a 0.20c' plain aileron which was internally sealed. The aileron extended from 0.614b/2 to 0.965b/2. The aileron hinge moments and the components of aileron normal force perpendicular to the wing chord line were measured by resistance type of strain gages mounted on each of the three beams connecting the aileron to the wing. A flexible seal was installed between the aileron and the wing. Twelve orifices, six above the seal and six below, were installed in the balance chamber to measure the pressure differential. The aileron details are shown in figure 1.

Details of the leading-edge and trailing-edge flaps are presented in figure 2. The leading-edge flaps had a constant chord of 3.05 inches measured normal to the leading edge of the wing and were deflected down 45° from the wing chord plane. The leading-edge flaps extended from 0.5b/2 to 0.975b/2.

The trailing-edge split flaps were made of $\frac{1}{16}$-inch duralumin and were deflected 60° from the lower surface of the wing measured normal to the 80-percent chord. They extended from the plane of symmetry to 0.4b/2 and the chord of the flaps equaled 20 percent of the wing chord perpendicular to the 0.286 chord line.

TESTS

The tests were made in the Langley 19-foot pressure tunnel with the air in the tunnel compressed to approximately $2\frac{1}{3}$ atmospheres. A Reynolds number of 6.0×10^6 and a Mach number of 0.14 were maintained during the tests. Measurements of the moments and forces were made for each configuration through the angle-of-attack range from -4° to approximately 30°. Aileron loads, hinge moments, and balance-chamber pressures were also obtained for each configuration from -20° to +20° aileron deflection.

CORRECTIONS TO DATA

The lift and pitching-moment data have been corrected for air-
stream misalinement and for support tare and interference effects. The
dynamic pressure has been corrected for the effects of blockage. Jet-
boundary corrections based on the method of reference 7 have been
applied to the angle of attack, pitching-moment coefficient, rolling-
moment coefficient, and yawing-moment coefficient. The rolling moments
obtained at $\delta_a = 0^0$ were used as tare corrections to the rolling
moments obtained at all aileron deflections and the tares applied are
shown in figure 3. Similar tares were applied to the yawing-moment
coefficients.

A calibration of the aileron seal indicated an average leakage
factor E of 0.12 due to the discontinuity of the seal along the
aileron span at the strain-gage beam positions and the leakage around
the ends of the ailerons. The resultant balance-chamber pressures at
each orifice station were corrected with corresponding E values to
obtain a simulated sealed condition. Leakage across the seal may have
an effect on the hinge moments and rolling moments at very low angles
of attack (reference 8). At moderate and high angles of attack, how-
ever, the effects of the leakage across the seal on the hinge moments and
rolling moments for the wing of the present investigation are believed to
be small.

The aileron-load coefficient was measured normal to the wing chord
for all deflection angles. An analysis of the aileron pressure distri-
bution data of reference 8, however, indicated that the chordwise forces
on the aileron are small; therefore the force normal to the aileron
chord line can be approximated by dividing C_{Z_a} by the cosine of δ_a.

RESULTS AND DISCUSSION

The basic aileron data are presented in figures 4 to 8. The results
have been summarized in figures 9 to 12.

Investigations of lateral control characteristics at low speeds and
high Reynolds numbers are of primary concern at high lift coefficients.
The rolling-moment data in the high-lift-coefficient range obtained in
the present investigation, however, exhibited scatter and nonlinearity
due to unsteady and unsymmetrical forces on the wing which resulted from
intermittent separated flow. Considerable vibration of the model also
occurred in the separated flow range, especially at angles of attack
near maximum lift.

In an effort to establish the reliability of the data, some retests
were made after the model and test apparatus were carefully checked, but
no appreciable difference in the nature of the results was obtained.
The rolling-moment variations which resulted from the unsteady forces,
as indicated in figure 3, were of smaller magnitude than the rolling
moments due to large aileron deflections (figs. 4(a), 5(a), and 6(a)).
Some degree of lateral control at high angles of attack would, there-
fore, be maintained. The aileron normal-force and hinge-moment data
do not exhibit the scatter which was obtained in the wing rolling-
moment data because the normal forces and hinge moments were recorded
visually from a highly damped self-balancing type of potentiometer.

From figures 3, 4(a), 5(a), and 6(a), it can be seen that the
rolling-moment oscillations were present for all aileron deflection
angles. The aileron, therefore, has little effect on the intermittent
separation characteristics, and the same difficulty in obtaining C_{l_δ}
would be experienced regardless of the aileron location or the type of
lateral-control device used.

It seems likely that vibrations similar to those experienced on
the wing of the present investigation may be induced on an airplane in
flight having a similar wing. The severity of the lateral oscillations
and vibrations for the wing cannot be predicted from the data obtained
from the present tests, however.

Previous investigations of wings of lower sweep having round-nose
airfoil sections have also shown nonlinearity and scatter of rolling-
moment data at angles of attack where flow was separated (references 1
and 2). The flow separation and accompanying irregularities of these
previous tests occurred at or near maximum lift; whereas in the present
investigation, separation occurred at an angle of attack well below
$C_{L_{max}}$, as indicated by figures 4, 5, and 6. The results obtained from
tests on the wing of the present investigation do not necessarily mean
that the same type of intermittent separated flow will be obtained on a
similar wing having a different airfoil section. Also, the intermittent
type of flow separation might be improved by the use of stall-control
devices other than those tested.

Rolling-moment characteristics.- Rolling-moment data are presented
for the entire angle-of-attack range tested; but the aileron effective-
ness parameter C_{l_δ}, as determined from a small range of aileron deflec-
tions through $\delta_a = 0^\circ$, was not evaluated for angles of attack greater
than 16° because of the scatter of data due to intermittent separated
flow in the higher angle-of-attack range. A C_{l_δ} value of about
0.00080 was obtained at 0° angle of attack for the plain wing (fig. 9).
A corresponding C_{l_δ} value of 0.00072 was calculated by the method of

reference 9. The aileron effectiveness decreased gradually as the angle of attack was increased from $0°$ to $16°$. With leading-edge flaps deflected, a value of C_{l_δ} of 0.00075 was obtained at zero angle of attack and remained fairly constant to about $12°$, beyond which it decreased. With both leading- and trailing-edge flaps deflected, C_{l_δ} was about 0.00080 at $0°$ angle of attack and remained approximately constant to an angle of attack of $9°$ and then decreased as the angle of attack was increased to $16°$.

At the angles of attack at which separation first occurred, as indicated by the unstable changes in the pitching moment (figs. 4(c), 5(c), and 6(c)), a large decrease in the rolling moment occurred for large negative (up) aileron deflection angles (figs. 4(a), 5(a), and 6(a)). The rolling moment for large positive (down) aileron deflections decreased gradually throughout the angle-of-attack range for the plain wing, decreased only in the high-lift-coefficient range with leading-edge flaps deflected, and remained approximately constant to maximum lift for the combination of leading- and trailing-edge flaps.

Comparisons of the rolling moments for various total aileron deflections are presented in figure 10. For total aileron deflections of $12°$ or more, the largest rolling moments were obtained below $5°$ angle of attack for the plain wing configuration. Between $5°$ and $16°$ angle of attack, the largest rolling moments were generally obtained with leading-edge flaps deflected, and beyond $16°$ the largest rolling moments were generally obtained with both leading- and trailing-edge flaps deflected. The rolling moments near the maximum lift coefficient for large total aileron deflection angles were about 70 percent of the values obtained at zero lift coefficient.

The yawing moments at small total aileron deflections were negligible through the angle-of-attack range for all configurations. As $\delta_{a_{total}}$ was increased, however, adverse yawing moments were obtained for all except very low angles of attack for each configuration. The variations of the yawing-moment coefficient with angle of attack for the highest total aileron deflection tested ($40°$) are shown in figure 10. The adverse yaw was greatest with the plain-wing configuration except at maximum lift coefficients.

Pitching-moment characteristics.- The effect of maximum up and down aileron deflections on the pitching-moment characteristics are presented in figures 4 to 6. The increments in pitching moment were larger for the up-aileron that for the down-aileron for all wing configurations except at angles below $4°$ for the plain wing and between $11°$ and $18°$ for the leading- and trailing-edge flap configuration, where the increments appeared to be equal. The dashed lines on the pitching-moment curves indicate the change in pitching moment due to

the combined maximum up and down aileron deflections for each wing con-
figuration. Deflection of the leading-edge flaps reduced the total
pitching-moment increment between the maximum up and down aileron deflec-
tions to about 70 percent of the corresponding plain-wing increment at
zero angle of attack. As the angle of attack was increased, the differ-
ence in total increments became smaller until they were about equal
at 20°. With the leading-edge flaps deflected, deflecting the trailing-
edge flaps increased the pitching-moment increment between the maximum
up and down aileron deflections throughout the angle-of-attack range.

Hinge-moment characteristics.- The parameters C_{h_δ}, C_{h_α}, $P_{R_{\dot{\delta}}}$,
and P_{R_α} are presented in figure 9 as functions of α. In order to
determine the hinge-moment characteristics in a steady roll, these
parameters have been utilized in the same manner as in reference 3:

$$C_{h_\delta}{}' = C_{h_\delta \text{ with balance}} + \frac{2(\Delta\alpha)_p}{\Delta\delta_a} C_{h_\alpha \text{ with balance}}$$

where

$C_{h_\delta}{}'$ rate of change of aileron hinge moment with deflection when
         wing is in a steady roll

$\dfrac{2(\Delta\alpha)_p}{\Delta\delta_a}$ ratio of effective change in angle of attack to total aileron
         deflection in a steady roll. (Values of this parameter as a
         function of wing and aileron geometric and aerodynamic
         characteristics are shown in reference 10. From these data
         the value of $\dfrac{2(\Delta\alpha)_p}{\Delta\delta_a}$ is found to be $-63.9 \dfrac{C_{l_\delta}}{C_{l_p}}$ or, with
         a value of C_{l_p} estimated from reference 11 to be 0.303,
         $\dfrac{2(\Delta\alpha)_p}{\Delta\delta_a} = -211 C_{l_\delta}$.)

The effects of the internally sealed balance are accounted for in the
following equations:

$$C_{h_\alpha \text{ with}} = C_{h_\alpha \text{ without}} + \frac{1}{2} P_{R_\alpha}\left(\frac{\bar{c}_b}{\bar{c}_a}\right)^2$$
$$\quad\quad\text{balance} \quad\quad\quad\quad \text{balance}$$

$$C_{h_\delta \text{ with}} = C_{h_\delta \text{ without}} + \frac{1}{2} P_{R_\delta}\left(\frac{\bar{c}_b}{\bar{c}_a}\right)^2$$
$$\quad\quad\text{balance} \quad\quad\quad\quad \text{balance}$$

where the span of the balance is assumed equal to the span of the
aileron and where the balance chord is assumed to include one-half of
the gap covered by the seal.

Values of C_{h_δ}' have been computed for several ratios of aileron
nose balance to aileron chord and are presented in figure 11 as a func-
tion of the angle of attack. For various balance chord ratios of the
plain-wing configuration, there was generally a small reduction in the
values of C_{h_δ}' as the angle of attack was increased from $0°$ to $12°$.
Between $12°$ and $16°$, however, values of C_{h_δ}' varied greatly with small
increments in angle of attack. At $14°$ angle of attack, a positive value
of C_{h_δ}' (overbalance) was obtained for zero balance chord ratio. The
overbalance resulted from the large negative value of C_{h_α} at $14°$, as
shown in figure 9. Although a large positive value of P_{R_α} also
occurred at $14°$, tending to counteract the effect of C_{h_α}, its effect
was small compared to the effect of C_{h_α}. It is believed that the large
values of both C_{h_α} and P_{R_α} for the plain wing at $14°$ angle of attack
resulted from the effects of vortex flow over the tip sections (refer-
ence 4). Deflection of the leading-edge flaps confined the vortex flow
to sections inboard of the leading-edge flap (reference 5), and hence
the large variations of C_{h_α} and P_{R_α} for the flaps-deflected configu-
rations were not obtained. Leading-edge flaps also tended to reduce the
variations of C_{h_δ} and P_{R_δ} with angle of attack at low lift coef-
ficients; consequently, the values of C_{h_δ}' were more nearly constant
with increase in angle of attack from $0°$ to $16°$. Figure 12 indicates
that a nose balance of approximately 60 percent of the aileron chord
will be required to balance the aileron below $12°$ angle of attack for
the plain wing or for leading-edge flaps deflected and below $16°$ angle
of attack for the combination of leading- and trailing-edge flaps
deflected.

Aileron-load characteristics.- The aileron coefficient C_{Z_a} (figs. 4(a), 5(a), and 6(a)) increased uniformly with angle of attack except for the plain wing, in which case a rather rapid increase occurred between 13° and 15° angle of attack. It is believed that the rapid increase in C_{Z_a} resulted from the effects of the vortex flow at the tips for the plain wing. The greatest values of C_{Z_a} were obtained with the configurations having flaps deflected.

CONCLUDING REMARKS

An investigation of a 20-percent-chord plain aileron on a 47.7° sweptback wing of aspect ratio 5.1 indicated the following:

1. Oscillations and vibrations of the wing at moderate and high angles of attack resulted from unsteady forces due to intermittent flow separation. The rolling-moment variations due to unsteady forces were smaller in magnitude, however, than the rolling moments due to large aileron deflections, thereby indicating that some degree of lateral control could be maintained throughout the lift-coefficient range. It is probable that vibration problems may be encountered on a wing of similar plan form and airfoil section in flight.

2. Although nonlinearity of rolling-moment data prohibited an evaluation of C_{l_δ} values at high lift coefficients the data indicated that for large total aileron deflections the rolling moments at maximum lift were about 70 percent of the values obtained at zero angle of attack.

3. The value of C_{l_δ} of 0.00080 for the plain wing at zero angle of attack was in fair agreement with the calculated value and the addition of leading- and trailing-edge flaps did not appreciably affect C_{l_δ} at low lift coefficients.

4. A ratio of the aileron nose balance to the aileron chord of 0.60 or more will be required to balance completely an internally sealed aileron of the type investigated.

Langley Aeronautical Laboratory
    National Advisory Committee for Aeronautics
        Langley Field, Va.

REFERENCES

1. Graham, Robert R., and Koven, William: Lateral-Control Investigation on a 37° Sweptback Wing of Aspect Ratio 6 at a Reynolds Number of 6,800,000. NACA RM L8K12, 1949.

2. Bollech, Thomas V., and Pratt, George L.: Investigation of Low-Speed Aileron Control Characteristics at a Reynolds Number of 6,800,000 of a Wing with Leading Edge Swept Back 42° with and without High-Lift Devices. NACA RM L9E24, 1949.

3. Spooner, Stanley H., and Woods, Robert L.: Low-Speed Investigation of Aileron and Spoiler Characteristics of a Wing Having 42° Sweepback of the Leading Edge and Circular-Arc Airfoil Sections at Reynolds Numbers of Approximately 6.0×10^6. NACA RM L9A07, 1949.

4. Salmi, Reino J., and Carros, Robert J.: Longitudinal Characteristics of Two 47.7° Sweptback Wings with Aspect Ratios of 5.1 and 6.0 at Reynolds Numbers up to 10×10^6. NACA RM L50A04, 1950.

5. Salmi, Reino J.: Effects of Leading-Edge Devices and Trailing-Edge Flaps on Longitudinal Characteristics of Two 47.7° Sweptback Wings of Aspect Ratios 5.1 and 6.0 at a Reynolds Number of 6.0×10^6. NACA RM L50F20, 1950.

6. Salmi, Reino J.: Horizontal-Tail Effectiveness and Downwash Surveys for Two 47.7° Sweptback Wing-Fuselage Combinations with Aspect Ratios of 5.1 and 6.0 at a Reynolds Number of 6.0×10^6. NACA RM L50K06, 1951.

7. Sivells, James C., and Salmi, Rachel M.: Jet-Boundary Corrections for Complete and Semispan Swept Wings in Closed Circular Wind Tunnels. NACA TN 2454, 1951.

8. Bird, J. D.: Effect of Leakage past Aileron Nose on Aerodynamic Characteristics of Plain and Internally Balanced Ailerons on NACA 66(215)-216, a = 1.0 Airfoil. NACA ACR L5F13a, 1945.

9. Lowry, John G., and Schneiter, Leslie E.: Estimation of Effectiveness of Flap-Type Controls on Sweptback Wings. NACA TN 1674, 1948.

10. Langley Research Staff (Compiled by Thomas A. Toll): Summary of Lateral-Control Research. NACA Rep. 868, 1947. (Formerly NACA TN 1245.)

11. Toll, Thomas A., and Queijo, M. J.: Approximate Relations and Charts
       for Low-Speed Stability Derivatives of Swept Wings. NACA TN 1581,
       1948.
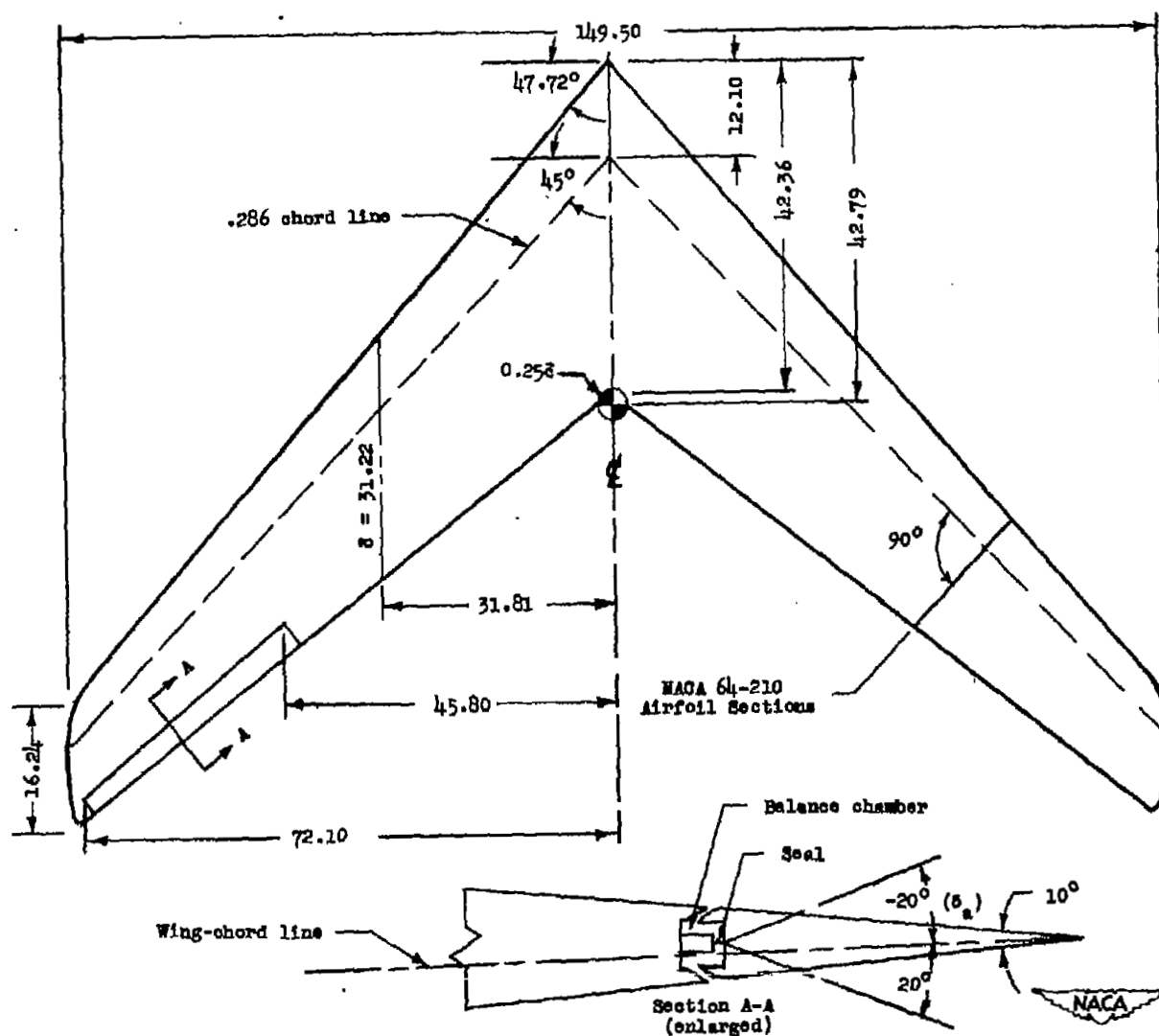
Figure 1.- Geometry of the wing and aileron details. All dimensions in inches. Aspect ratio, 5.1; taper ratio, 0.383.

Figure 2.- Details of high-lift and stall-control devices.

Wing chord line.

3.05"

45°

$\frac{1}{2}"$ D

Section A-A

Leading-edge flaps.

Wing chord line.

60°

.20"
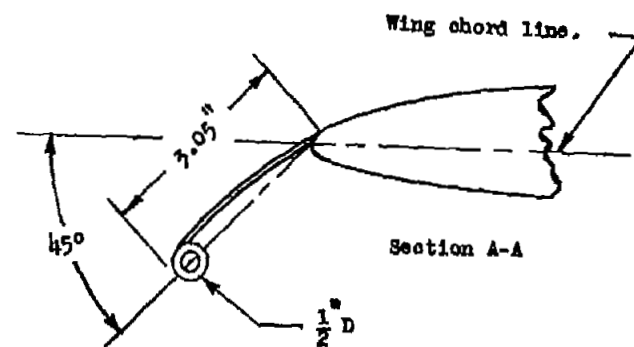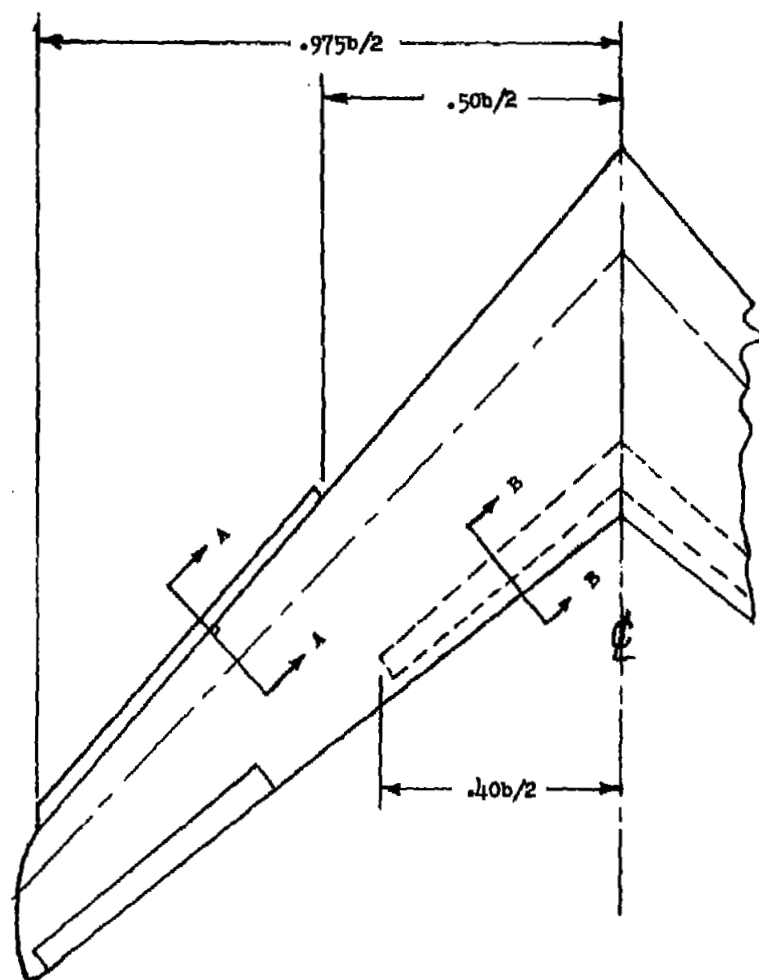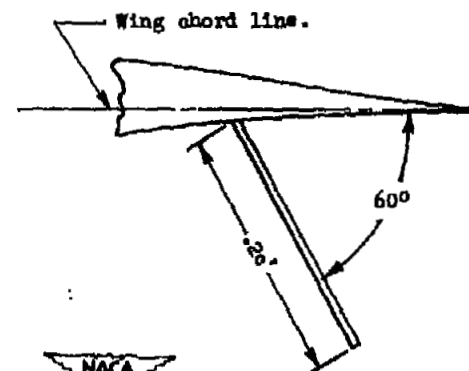
Section B-B

Split flaps.
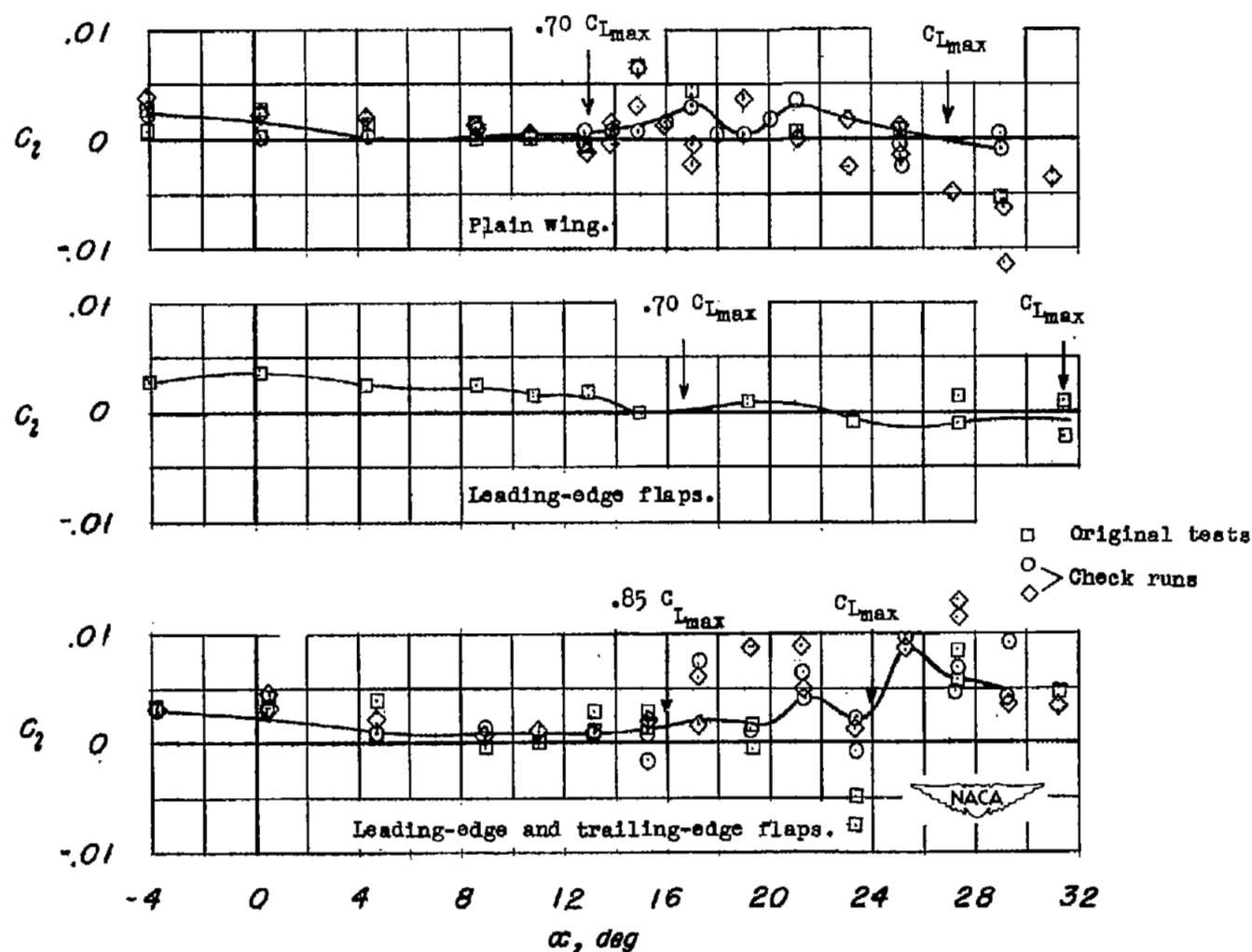
Figure 3.- Variations of rolling-moment coefficient with angle of attack for zero aileron deflection. Faired curves represent tare corrections for the three model configurations tested.
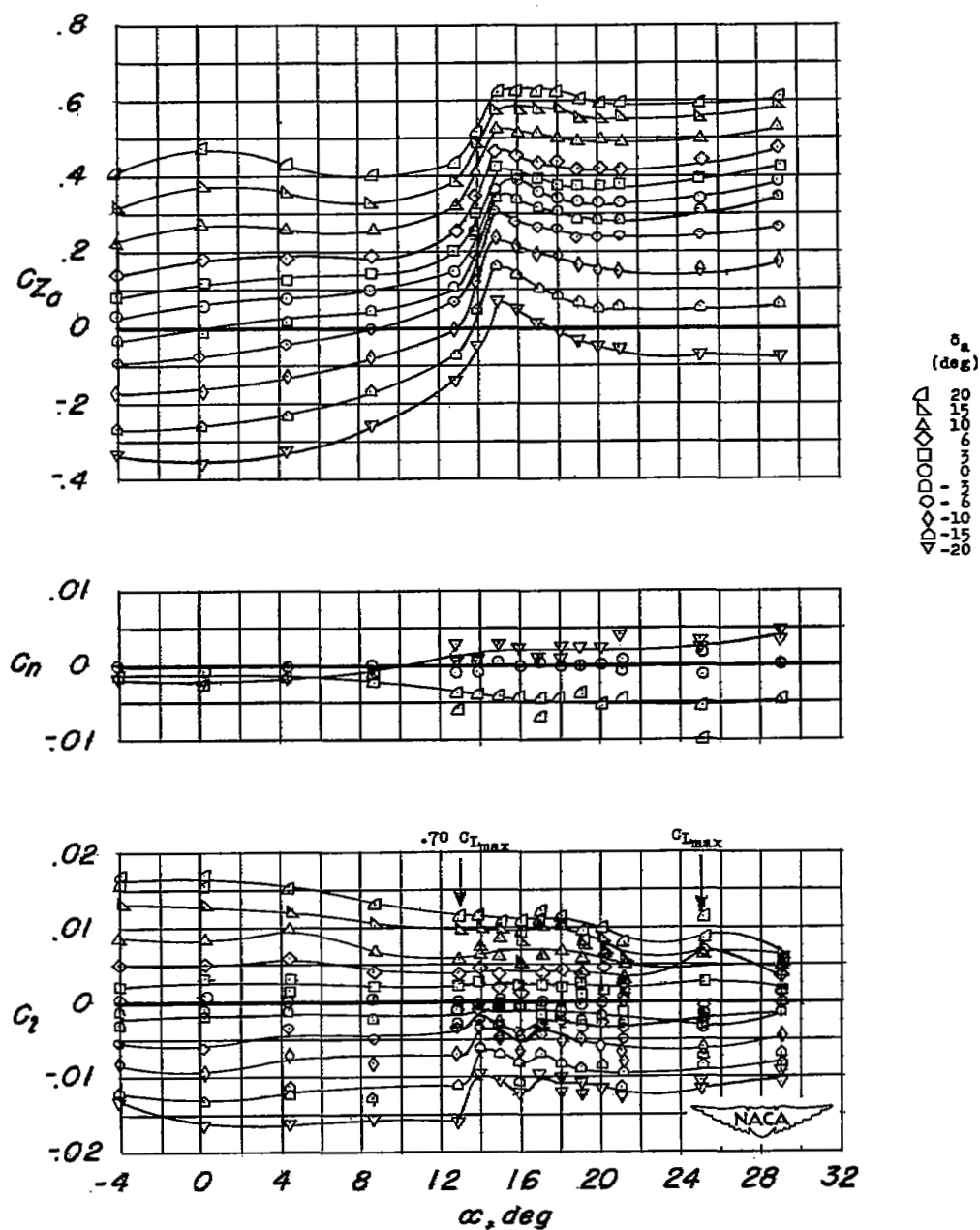
(a) C_{Z_a}, C_n, and C_l against α.

Figure 4.- Aileron characteristics of the plain wing.
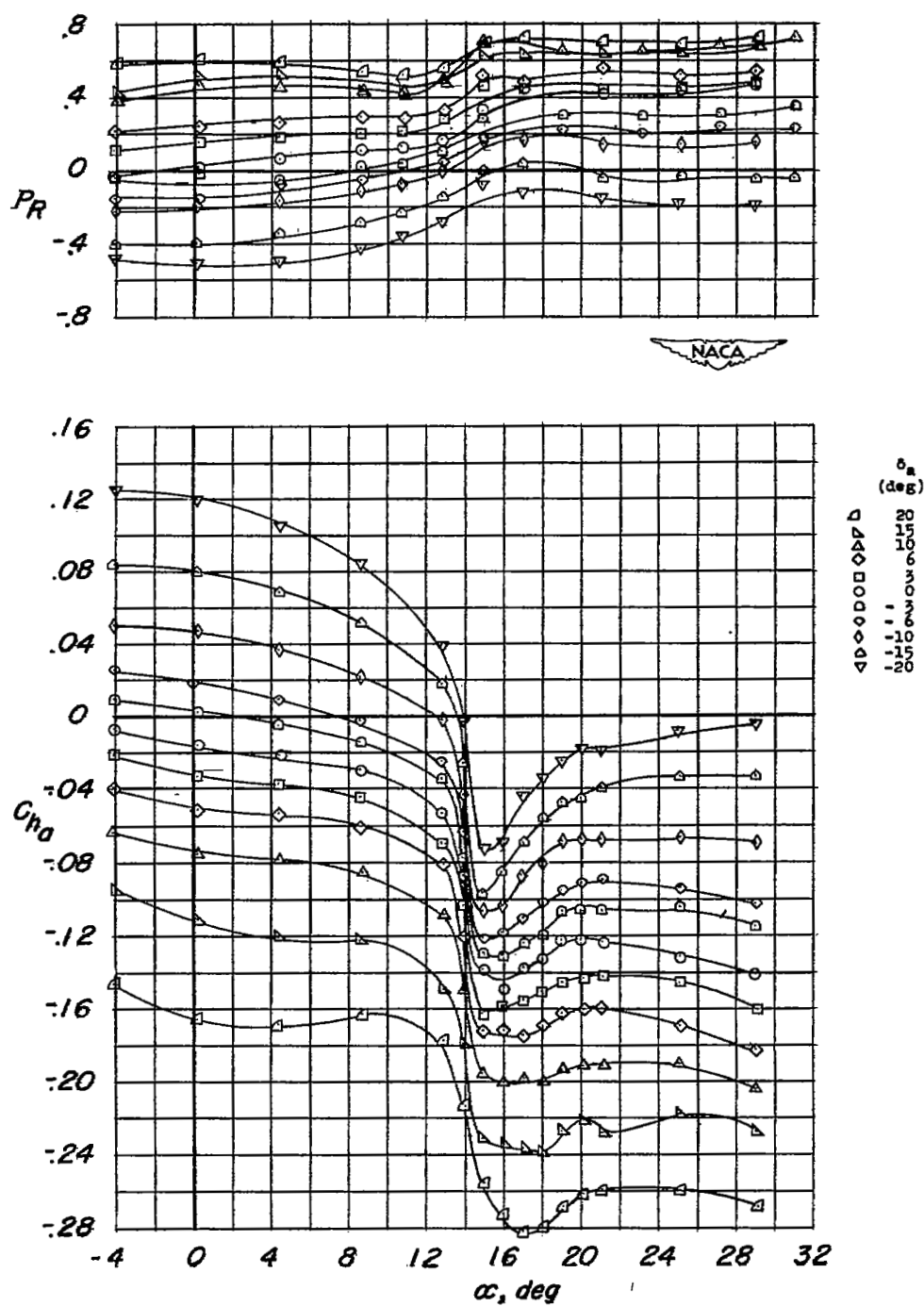
(b) P_R and C_{h_a} against α.

Figure 4.- Continued.
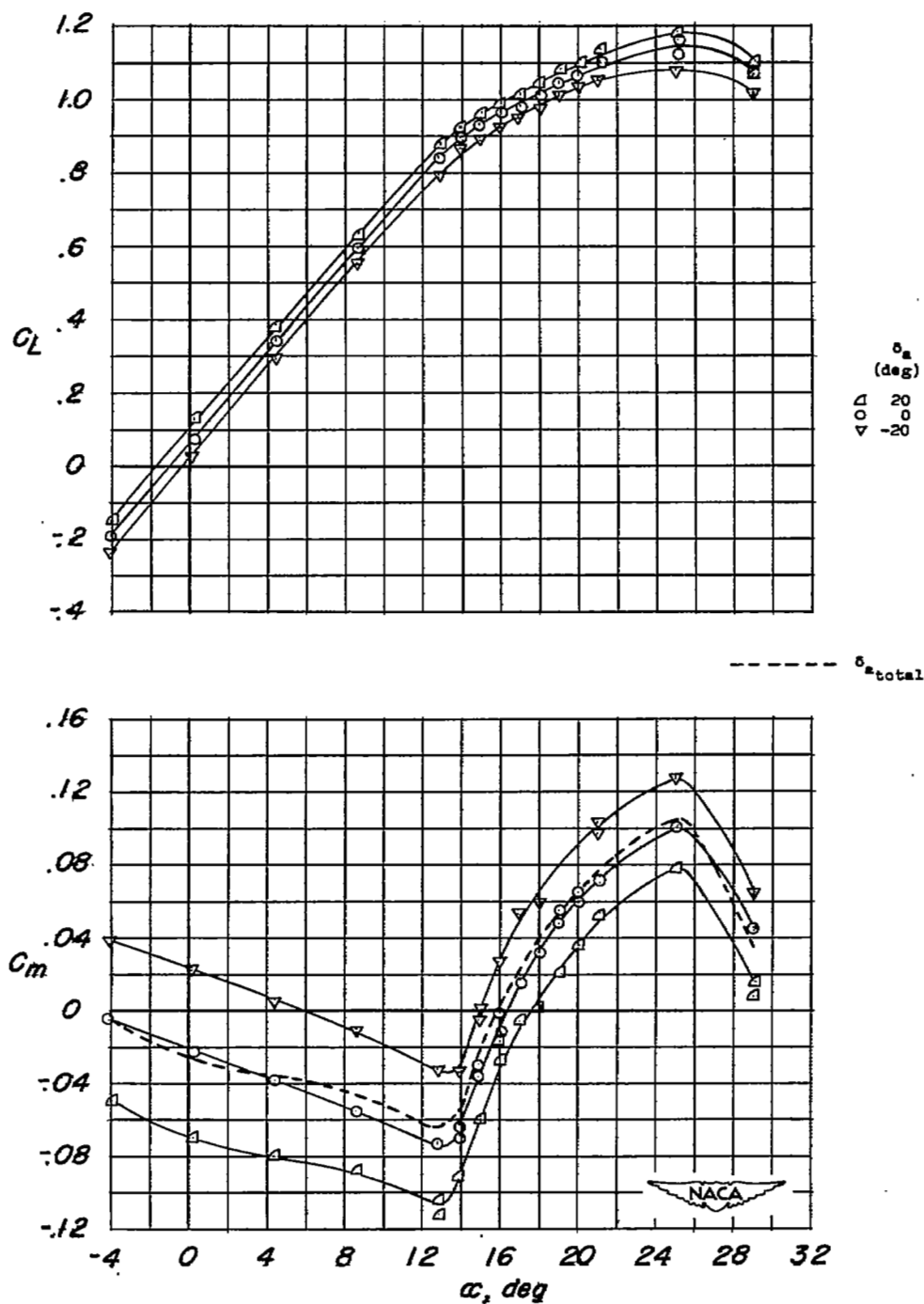
(c) C_L and C_m against α.

Figure 4.- Concluded.
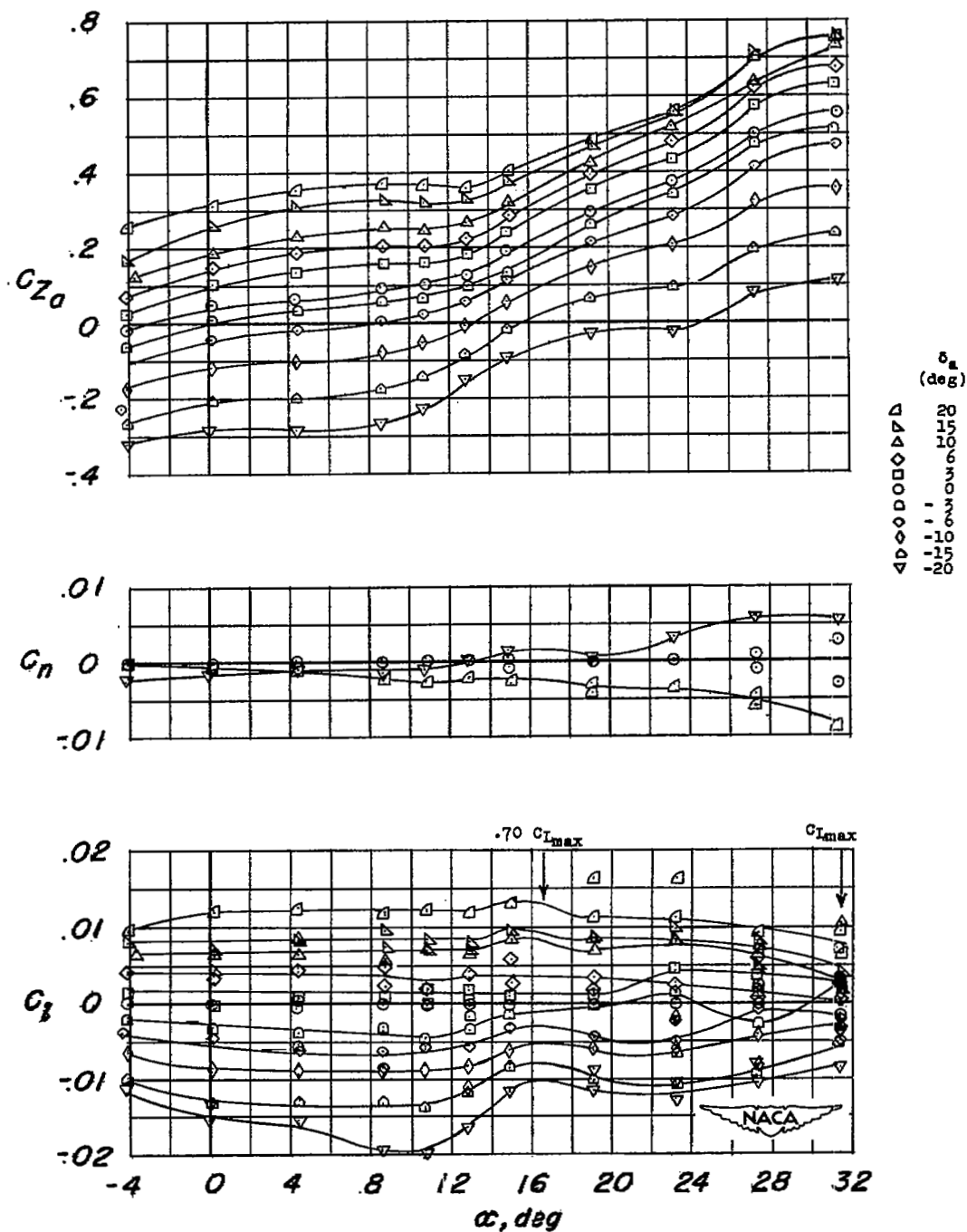
(a) c_{Z_a}, C_n, and C_l against α.

Figure 5.- Aileron characteristics of the wing with leading-edge flaps
deflected.
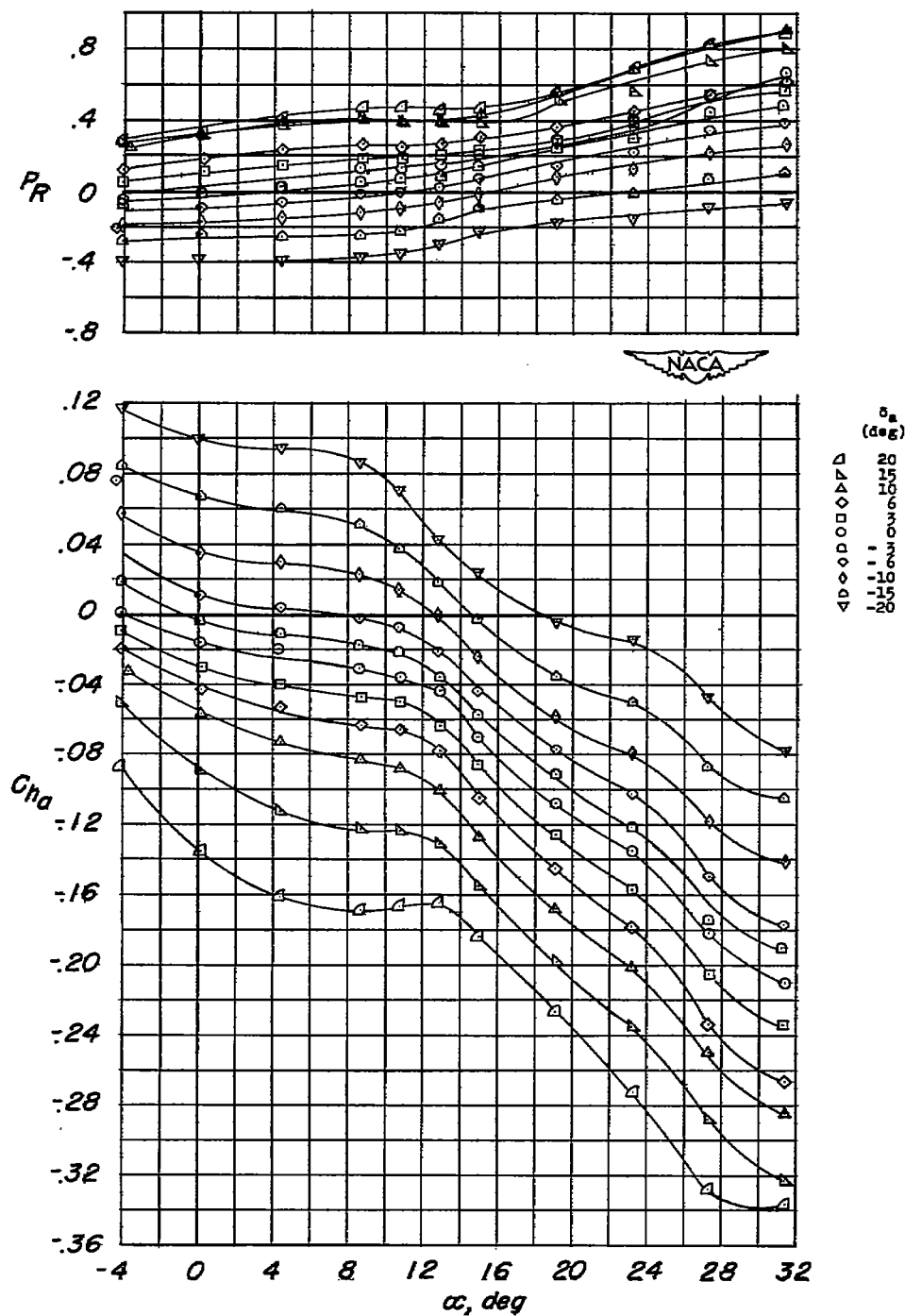
(b) P_R and C_{h_a} against α.

Figure 5.- Continued.
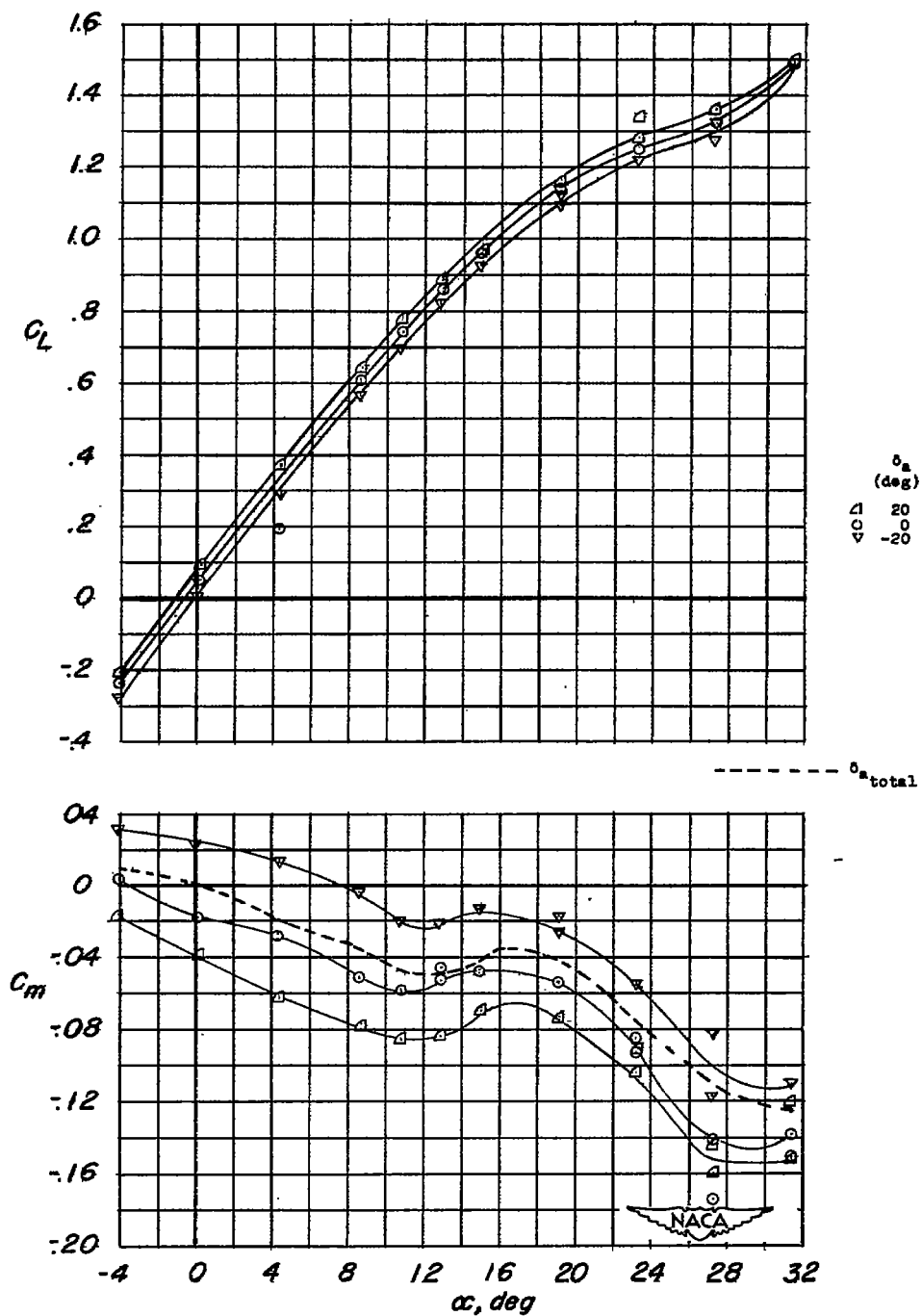
(c) C_L and C_m against α.

Figure 5.- Concluded.
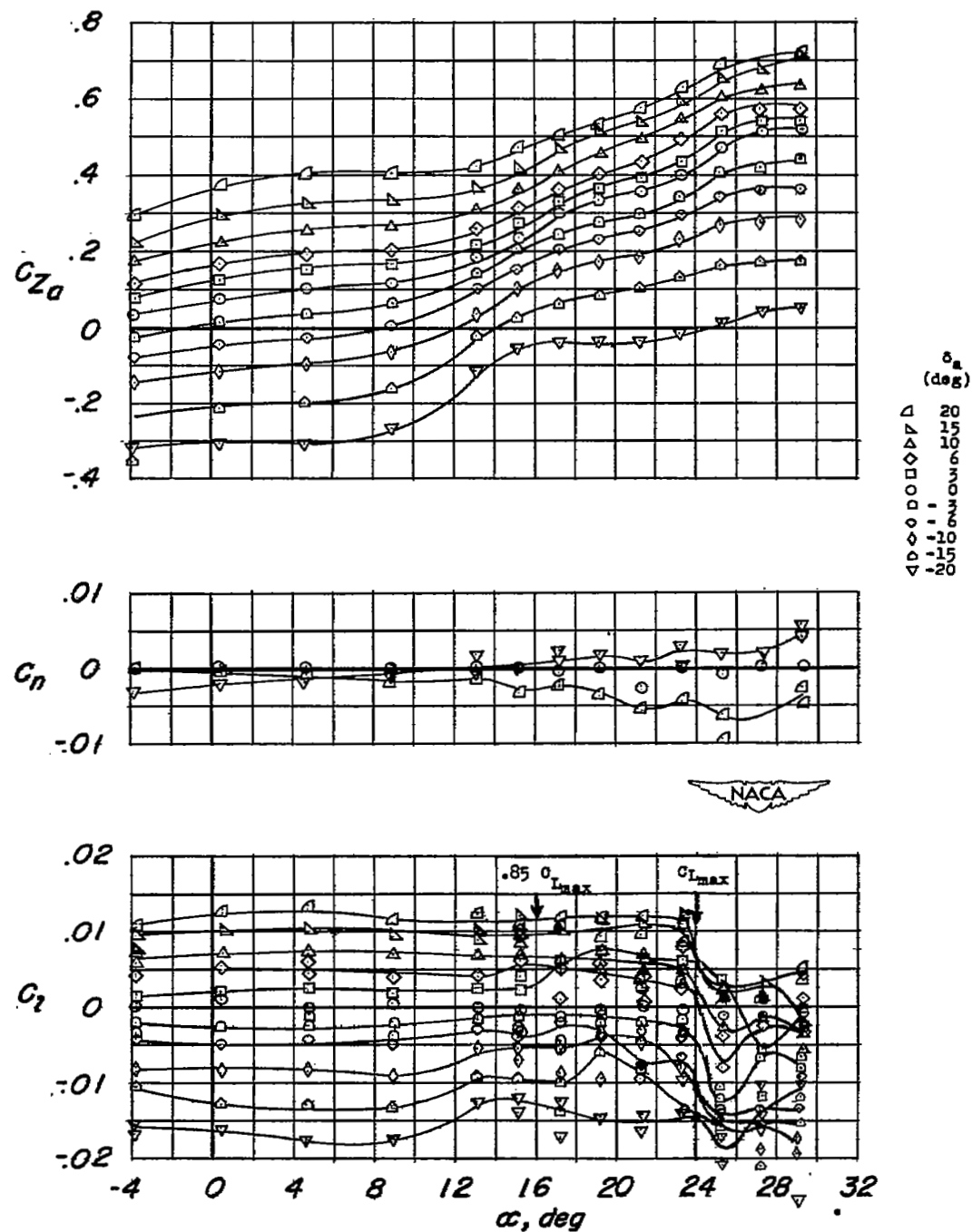
(a) c_{Z_a}, C_n, and C_l against α.

Figure 6.- Aileron characteristics of the wing with leading- and trailing-
edge flaps deflected.
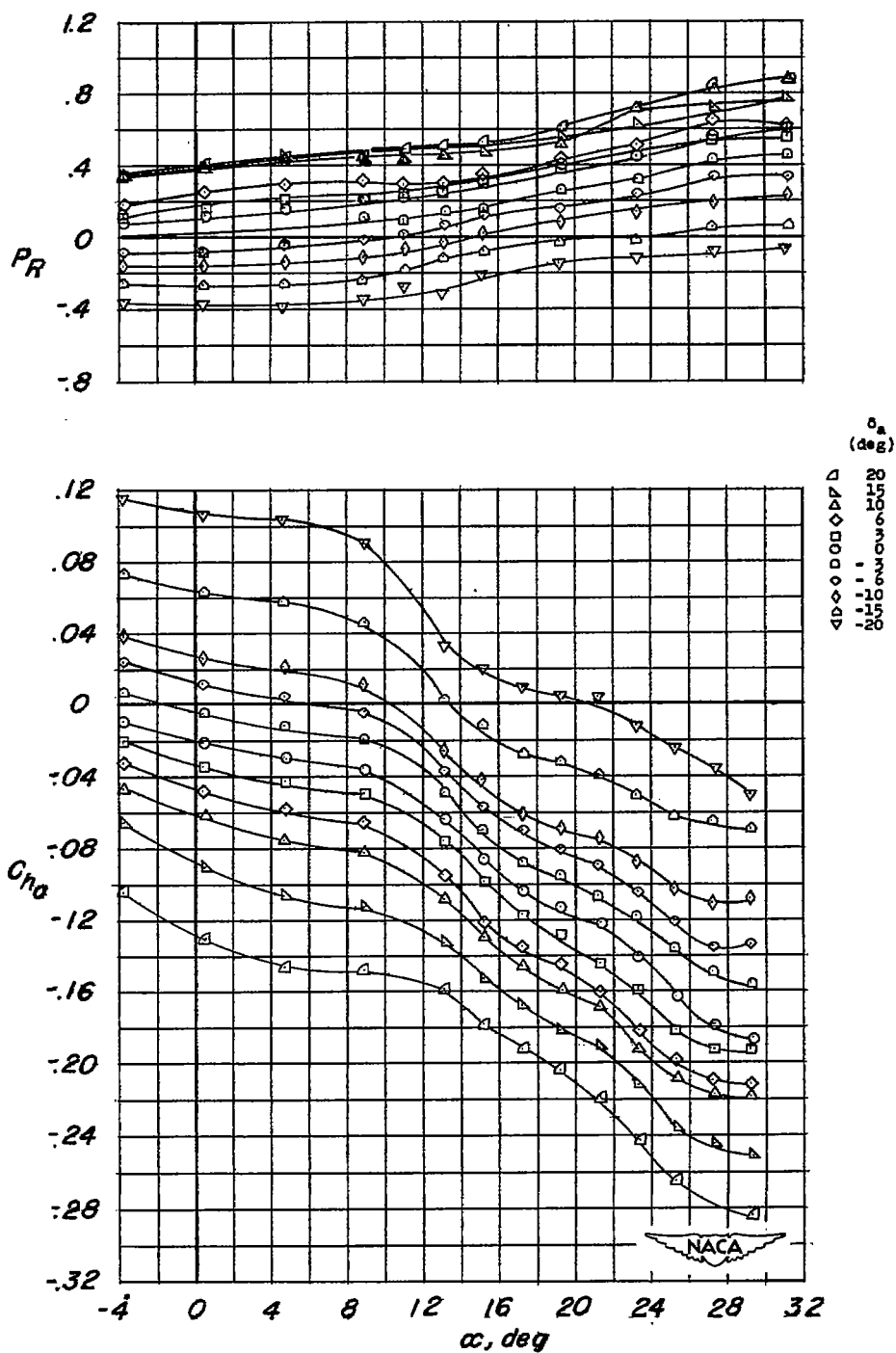
(b) P_R and C_{h_a} against α.

Figure 6.- Continued.
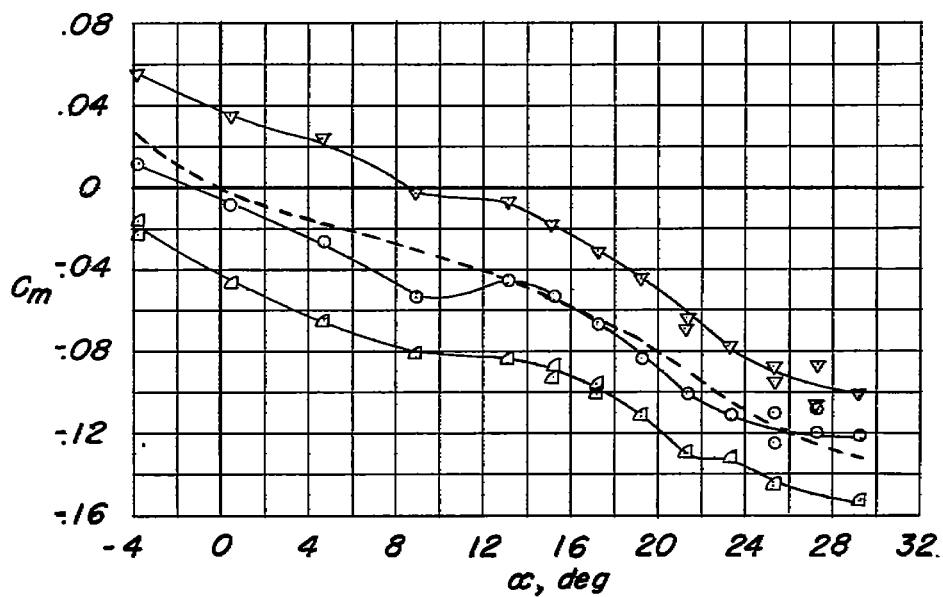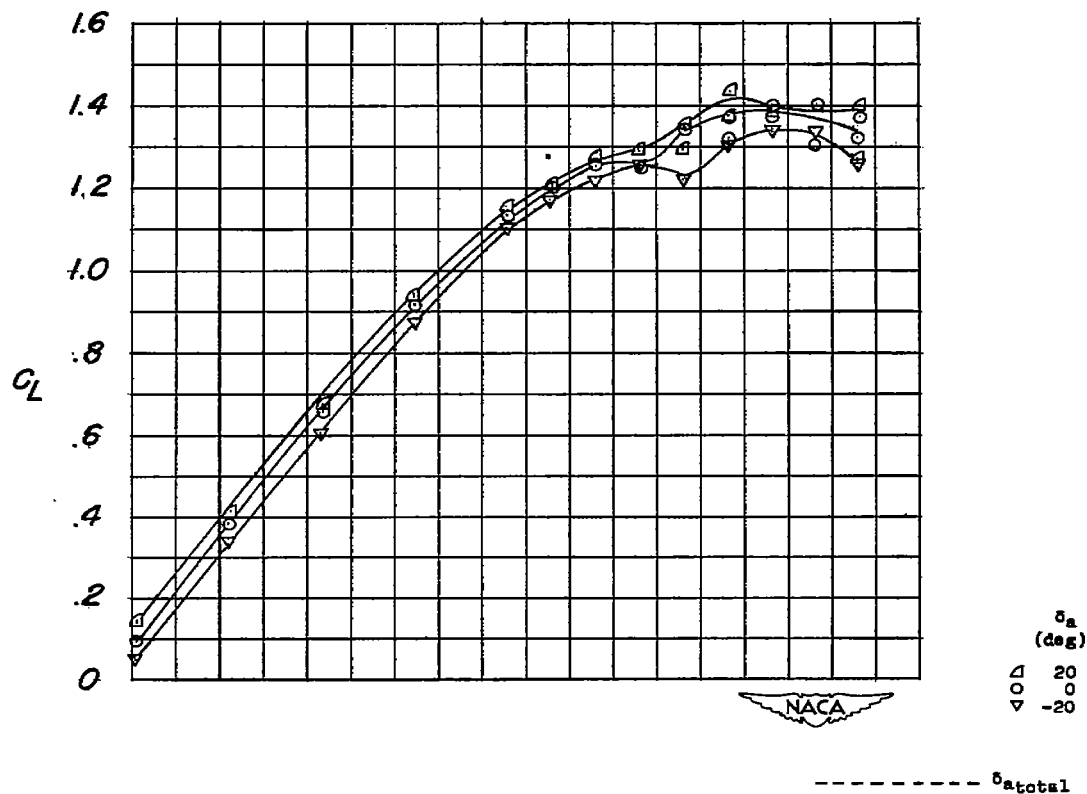
(c) C_L and C_m against α.

Figure 6.- Concluded.
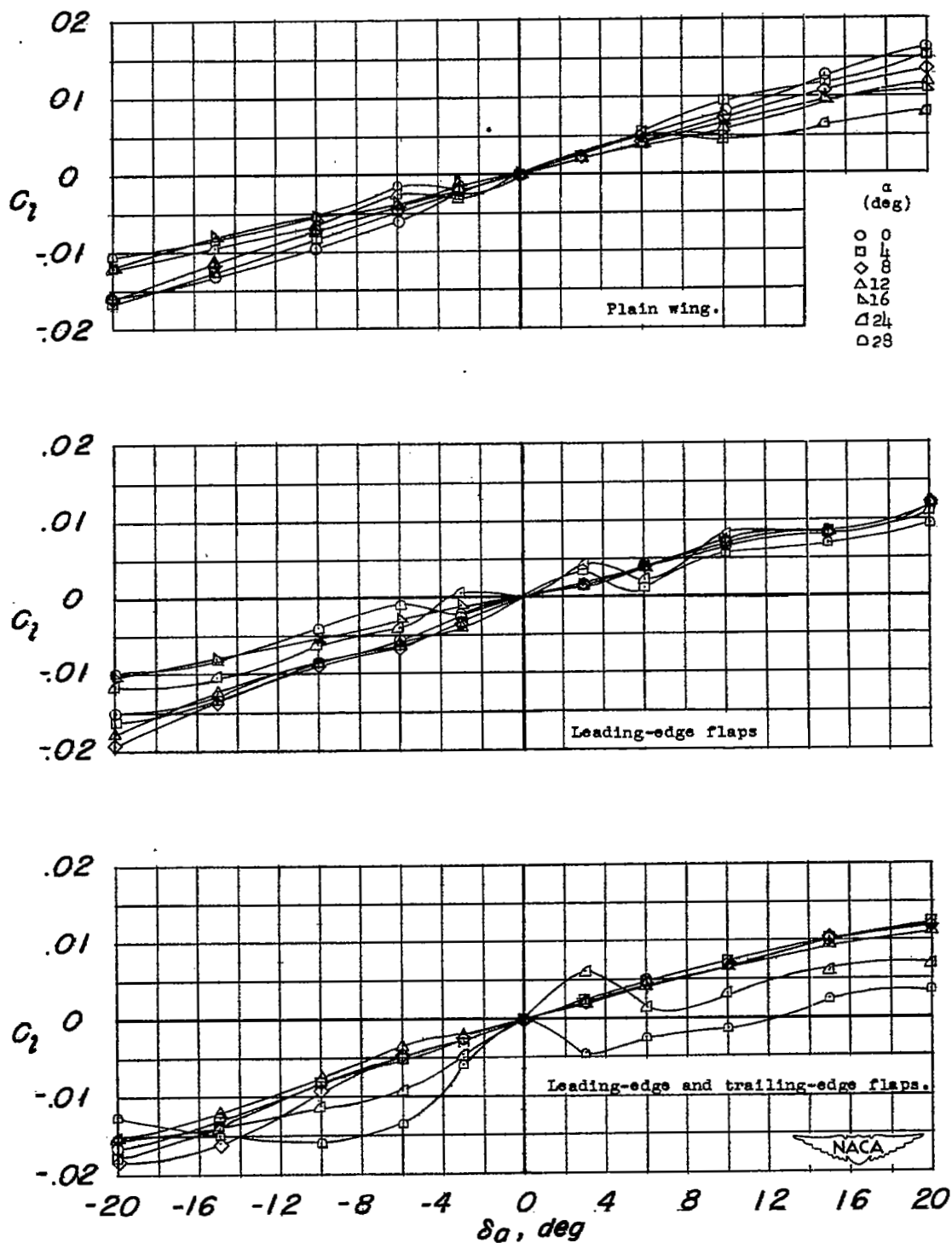
Figure 7.- The variation of rolling-moment coefficient with aileron deflection for various model configurations.
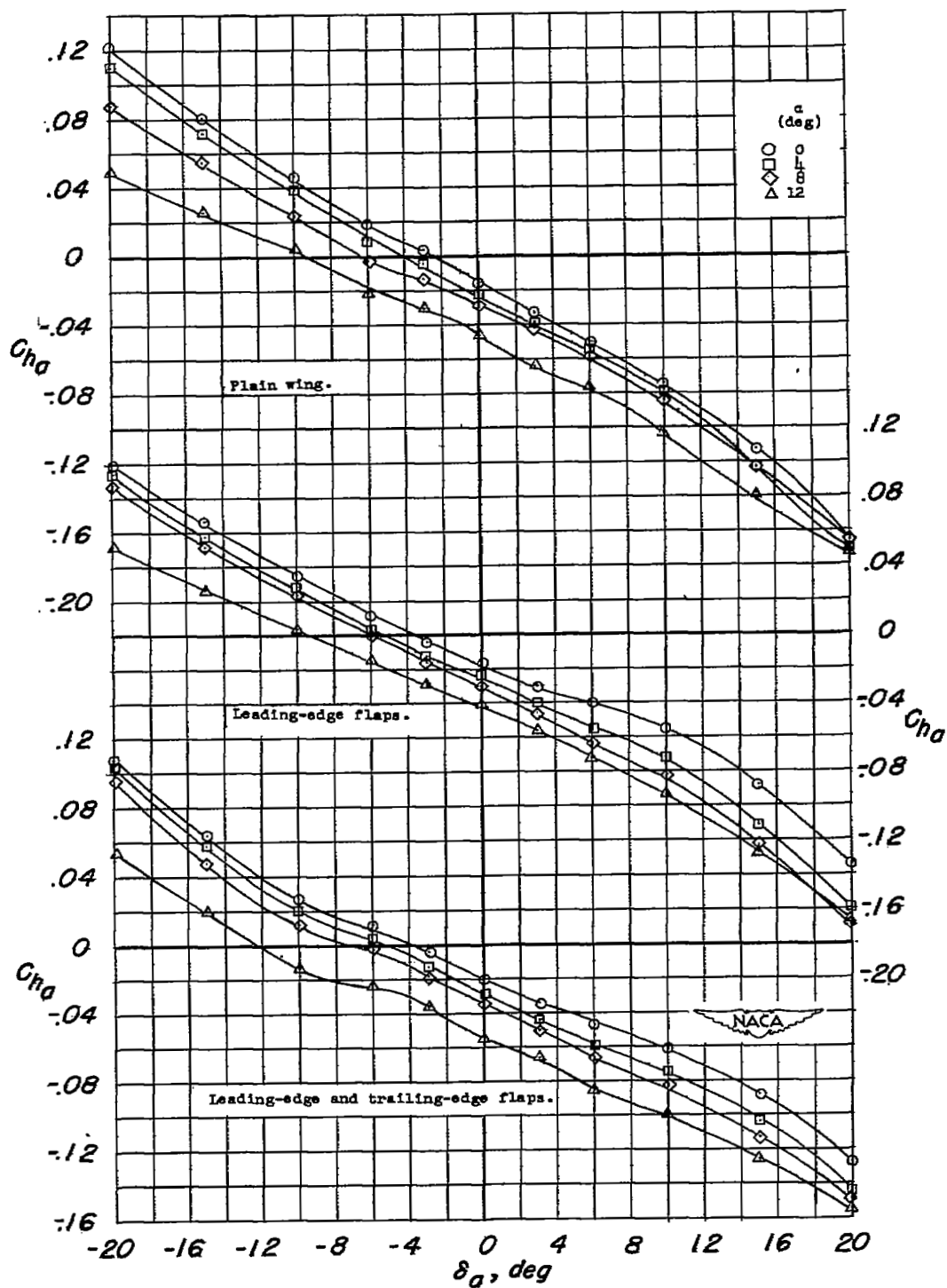
Figure 8.- The variation of aileron hinge-moment coefficient with aileron
deflection for various model configurations.
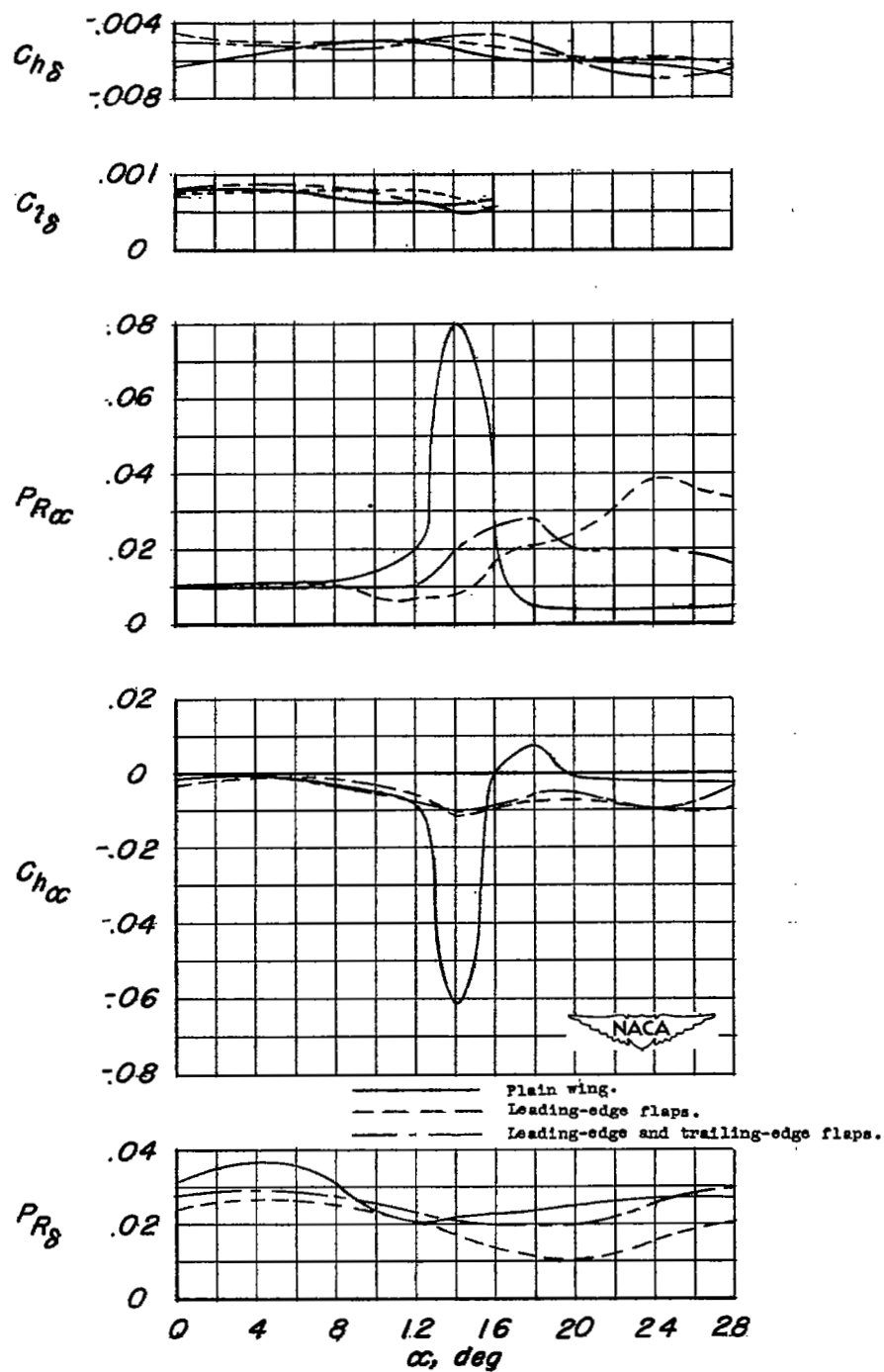
Figure 9.- The effects of high-lift and stall-control devices on the aileron hinge-moment and effectiveness parameters C_{h_δ}, C_{l_δ}, P_{R_α}, C_{h_α}, and P_{R_δ}.
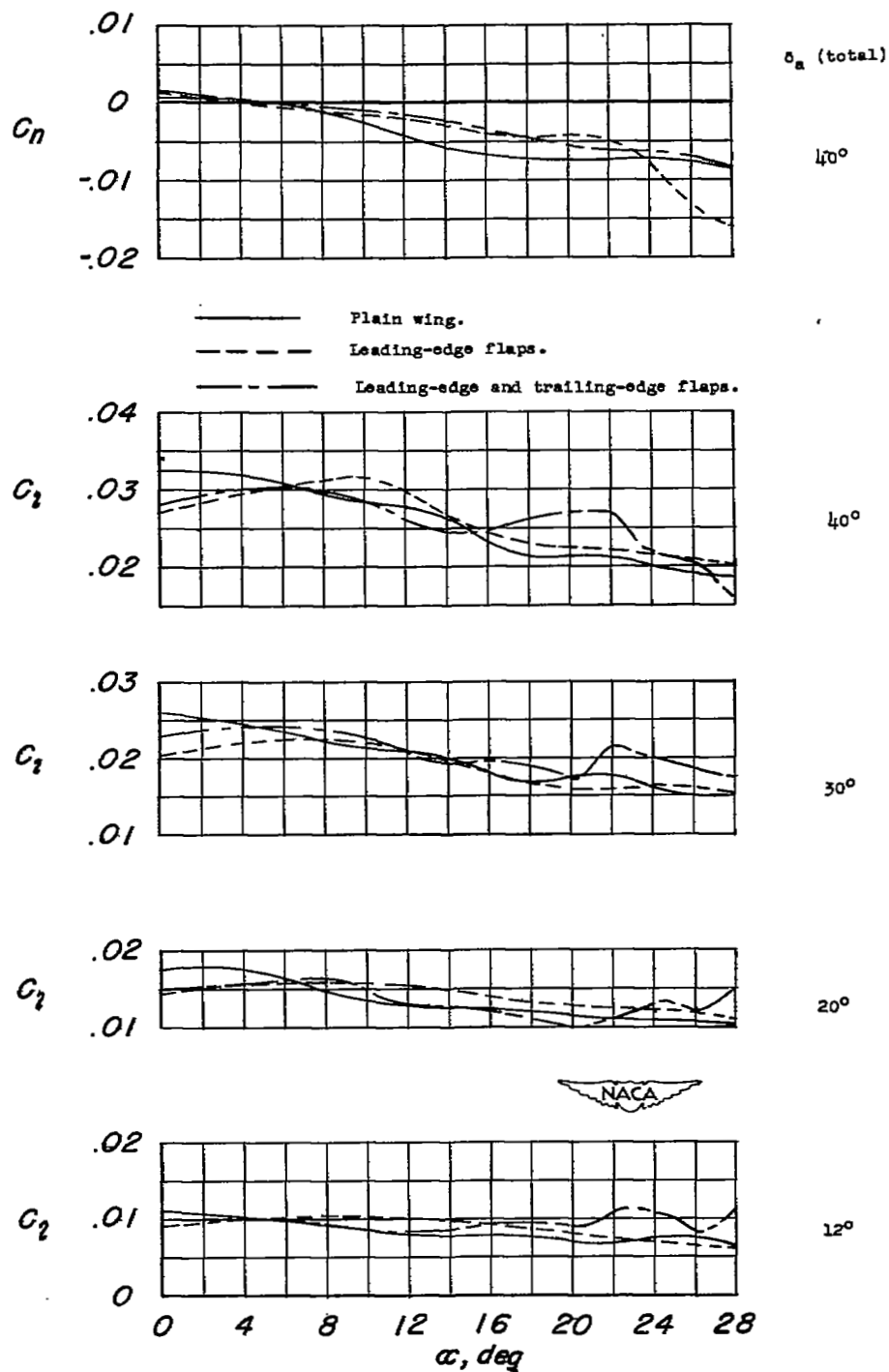
Figure 10.- Variation of rolling-moment and yawing-moment coefficients
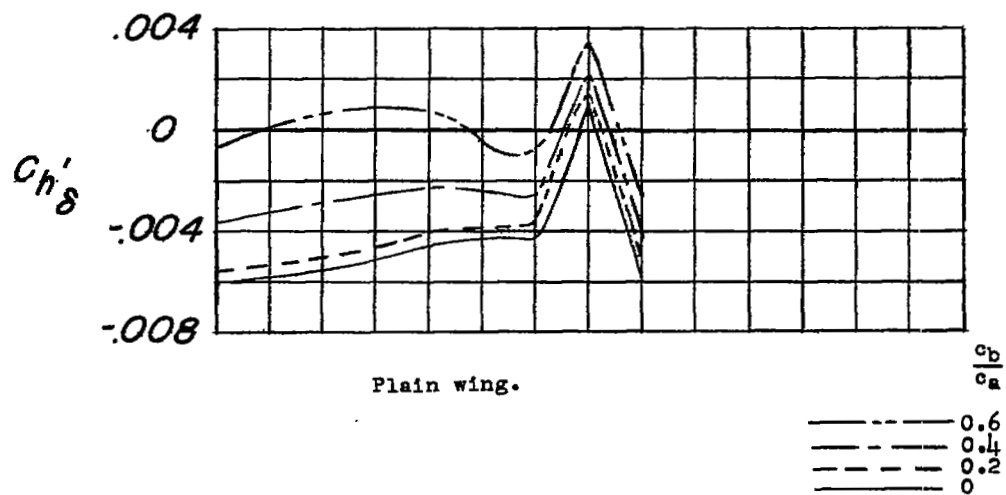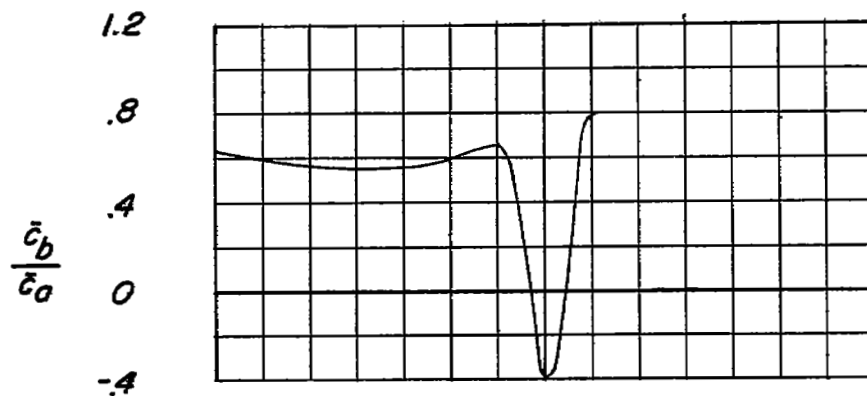with angle of attack for several model configurations and total aileron
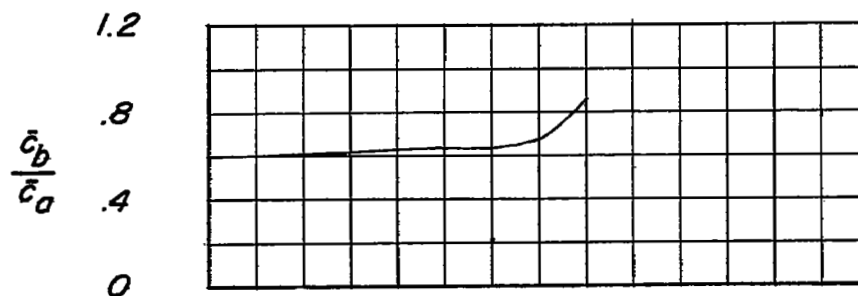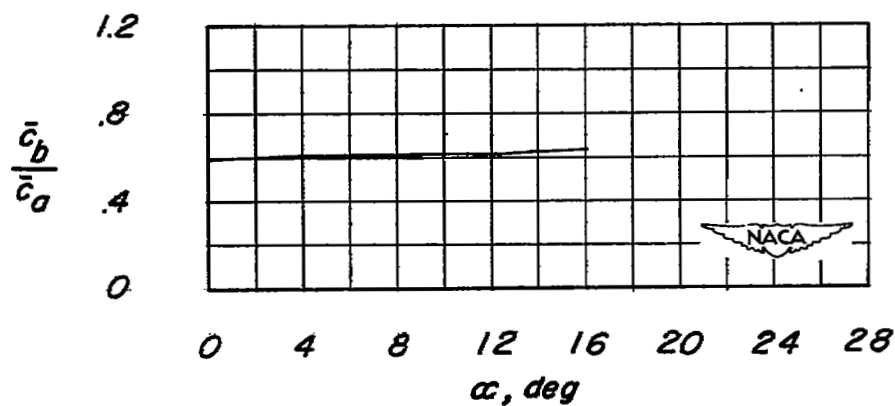deflections.
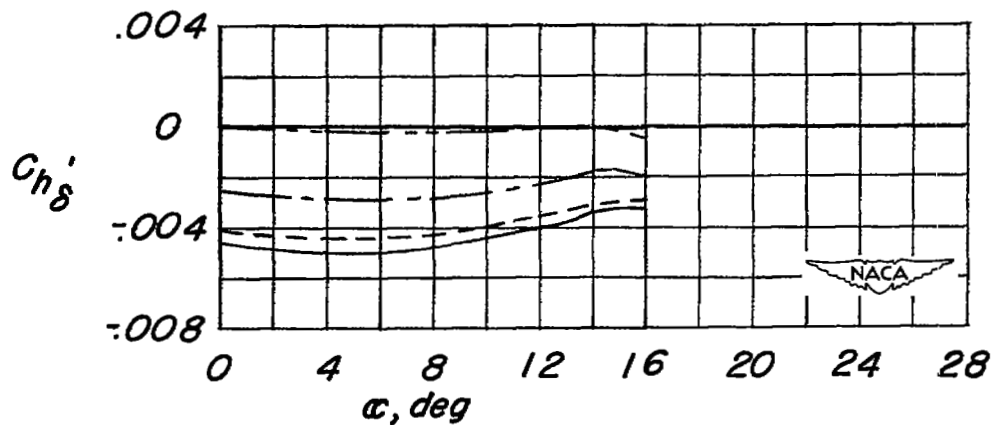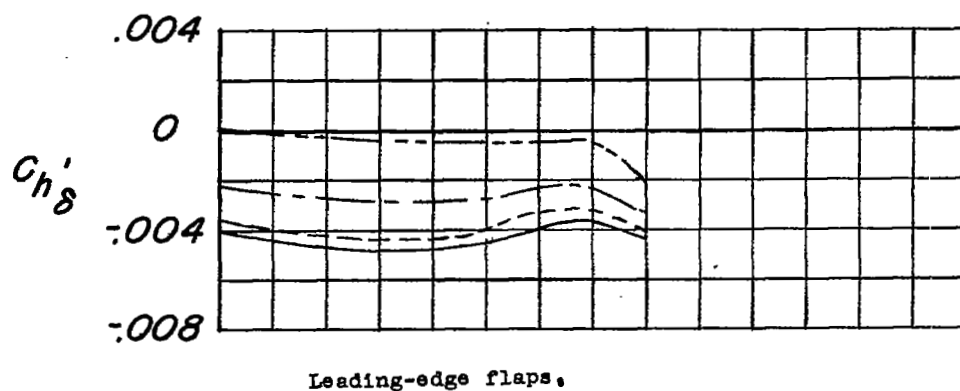
Figure 11.- The effect of various amounts of aerodynamic balance on the
aileron hinge-moment parameter C_{h_δ}'.

Plain wing.

Leading-edge flaps.

Leading-edge and trailing-edge flaps.

α, deg

Figure 12.- Variation of aileron balance chord ratio with angle of attack for zero stick force in a steady roll.